Journal of Electronic Research and Application, 2021, Volume 5, Issue 4
http://ojs.bbwpublisher.com/index.php/JERA
ISSN Online: 2208-3510
ISSN Print: 2208-3502

Summary of the Performance of V_2O_5 Materials as Lithium Battery Cathode

Weihao Wang*

Room 1303, Building 69, 66 Gulong Road, Shanghai 201102, China

***Corresponding author:** Weihao Wang, isaac_wang2004@126.com

Abstract: Lithium battery has recently gained more and more attention worldwide. It has wide usage that range from toys to electric cars. Choosing a suitable material that best fits the overall performance as electrode for the battery is very essential. For cathode material, apart from the traditional and widely-used $LiCoO_2$, $LiFePO_4$ and so on, there are innovations that include the use of V_2O_5. Researches have been done focusing on how to further improve the performance for V_2O_5 cathode in terms of different structure, forms or combination with other chemical molecules. This research paper will make a summary of the materials derived from traditional V_2O_5 as well as their performances.

Keywords: Lithium battery; Cathode material; V_2O_5 materials and performance

Publication date: July 2021; ***Online publication:*** July 31, 2021

1. Introduction

The development of high-performance lithium ion batteries is mainly limited by the relatively low capacity of the negative electrode and poor cycling stability. Considering the limitations of $LiCoO_2$, $LiMn_2O_4$ and other traditional cathode materials, the low theoretical capacity and multi-step synthesis requirements of $LiFePO_4$, these materials do not have advantages for flexible wearable electronic devices in the new era [1-2]. However, a new type of cathode material V_2O_5 with high theoretical specific capacity and abundant activity in nature appears to be a very appealing choice. V_2O_5 has a variety of derived materials which make it has a great research prospect. Vanadium-based compounds exhibit a range of oxidation states, including V^{5+}, V^{4+}, V^{3+}, and V^{2+}, making them feasible to composite with many other anions and cations to form vanadium oxides [3].

Poor cyclic performance is the most important problem for V_2O_5 materials and its derivatives. The most serious problem for traditional lithium battery cathode materials is that the long cycle stability, good rate capability, and high mass loading cannot be achieved at the same time [4], which is caused by the irreversible Li^+ intercalation at the deep discharge condition

In this passage, several different materials derived and improved from the original vanadium oxides compound in terms of their performance are concluded. These materials include V_2O_5 with HoMSs, O vacancies and so on, while also in different forms, such as in xerogel forms and in nanotube form. Many of them have significant improvement compared with traditional form considering in charge-discharge capacity and other means, but meanwhile perform poorer in other aspects, especially in the performance of stable cyclability.

2. Materials and Performances

2.1. V_2O_5 Nanotubes

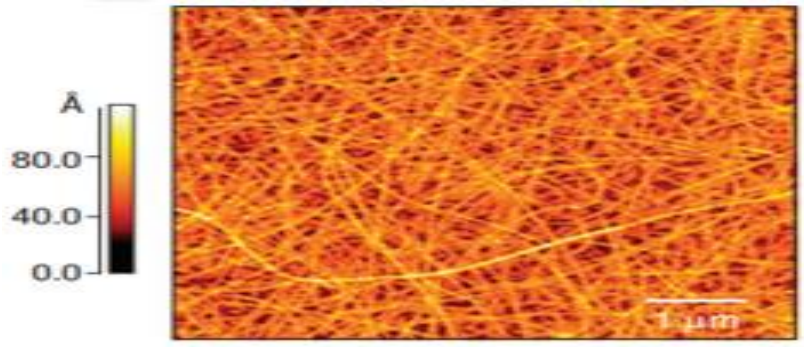

Figure 1. Images of V_2O_5 nanofiber [5]

V_2O_5 nanotube array has initial capacity of 300 mA h g^{-1}, which is almost two times higher compared to the initial capacity of the traditional V_2O_5 film, which is 140 mA h g^{-1}. Short diffusion distance and large surface area of the nanotube array are the main reasons for this improvement in capacity.

However, unstable discharge cyclability performance is still obvious (the capacity is reduced to 2001and 180 mA h g^{-1} at the second and third charge and discharge), but there is still improvement compared with colloidal or ordinary V_2O_5 film (30% more power than traditional V_2O_5 film at the sixth charge and discharge) [5-6].

Newly reported improvement related to V_2O_5 Nanofibers includes V_2O_5/CNT (Carbon nanotube). **Figure 2.** shows the number of cycles in the relation with capacitance retention. V_2O_5/CNTs composites have good electrochemical stability, and after 5000 cycles, the capacitance loss is only 8.8%, which is a high result compared with other electrodes.

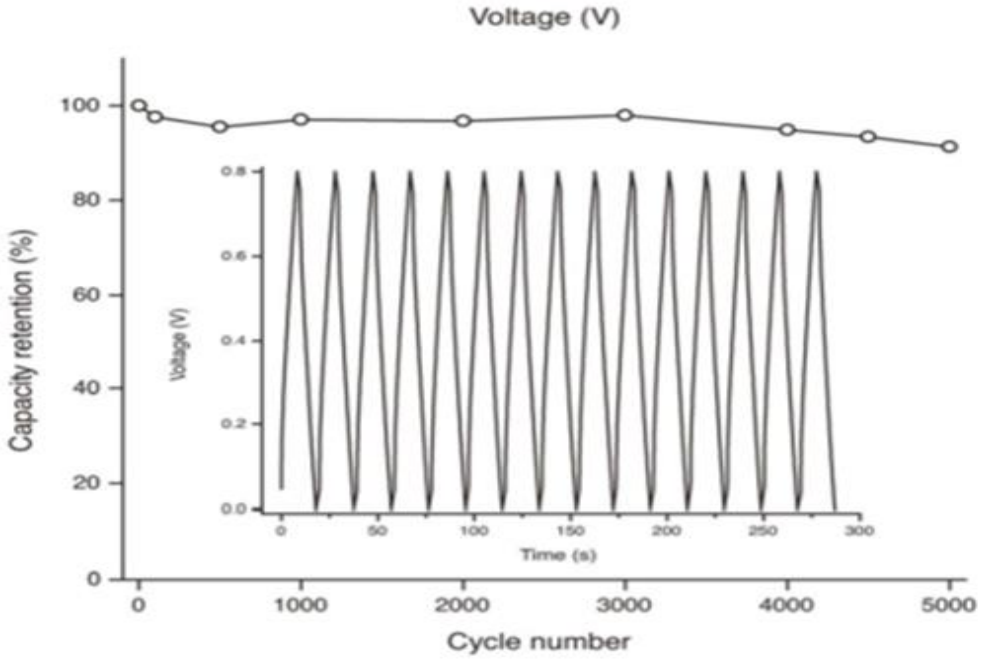

Figure 2. V_2O_5/CNTs capacity retention in relating with cycle numbers [6]

It was found that V_2O_5 /CNTs with weight ratio 0.5:1 had the highest capacitance among different ratios. Due to mutual penetration of carbon nanotubes and V_2O_5 nanosheets, the composite structure is layered porous. Based on the structure of V_2O_5, the conductivity of CNTs and the high capacity of V_2O_5,

V_2O_5 /CNT electrode has a power density (0.27 W cm^{-3}) and energy density (1.47 mWh cm^{-3}) [7].

2.2. V_2O_5 HoMSs (3D hollow multi-shelled structures)

The HoMSs, also known as 3D hollow multi-shelled structures, has more active sites and more surface-volume ratio can be provided for lithium-ion storage to improve the specific capacity of cathode. In addition, due to the shorter path needed to transport lithium electrons and ions and increased electrode-electrolyte contact area, HoMSs can make lithium ions enter lithium ions better, thus improving the rate capacity.

A 3D textile-based cathode electrode coupling a V_2O_5-HoMSs active material with a metal fabric collector for good quality flexible lithium batteries has been reported by Zhu et al., [8]. The cathode electrode of the fabric is composed of single or multi-shell V_2O_5 HoMSs synthesized by STA (denoted as nS- V_2O_5. The number n representing number of shells) for the active material, and cotton coated by nickel (reduced to Ni-Cotton) fabric for the use of mechanical support and conductive collector. Due to the advantages of the above HoMSs, the large surface area and flexibility shown of the Ni-Cotton structure, as well as the good combination of V_2O_5 HoMSs and Ni-Cotton, the 3S- V_2O_5 HoMSs/ Ni-Cotton electrode under the high-quality load of 2.5 mg cm^{-2}, it can maintain an astonishing capacity of 222.4 mA h g^{-1} even after 500 charge and discharge cycles. This proved that it has good ability for repeated use, also solving the traditional problem of cathode material in terms of poor cyclability.

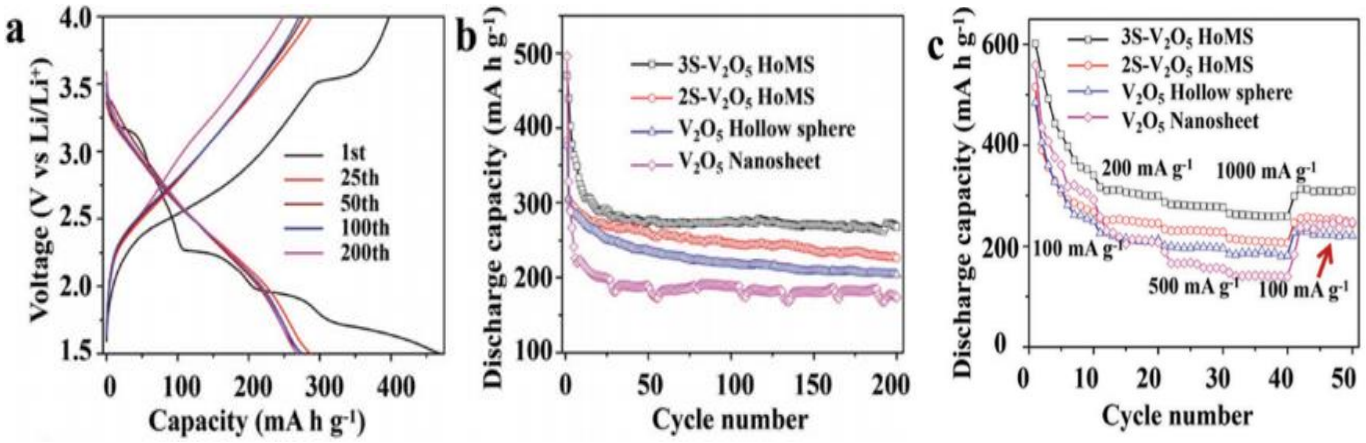

Figure 3. Note that V_2O_5 Hollow sphere also known as 1S-V_2O_5

Figure 3., Note that V_2O_5 Hollow sphere also known as 1S-V_2O_5 HoMS a) 1st, 25th, 50th, 100th, and 200th charge–discharge curves of 3S-V_2O_5 HoMSs/Ni-cotton. b) Cycling performance, measured at a current density of 500 mA g^{-1}, of V_2O_5 hollow sphere/Ni-cotton, 2S-V_2O_5 and 3S-V_2O_5 HoMSs/Ni-cotton, and V_2O_5 nanosheets/Ni-cotton fabric electrodes. c) Rate performance of V_2O_5 hollow spheres/Ni-cotton, 2S-V_2O_5 and 3S-V_2O_5 HoMSs/Ni-cotton, and V_2O_5 nanosheets/Ni-cotton fabric electrodes [8].

As shown in **Figure 3.** c, specific discharge capacity of 3S-V_2O_5 HoMSs electrode was 601.8 mAh g^{-1} under current density of 100 mA g^{-1}. That is much better compared with other traditional cathode material. Even when the current density increased to 1000 mA g^{-1}, there is still a high capacity of 264.6 mA h g^{-1}.

In **Figure 3.** b, the capacities of HoMSs and nanosheets after 200 cycles were respectively 268.3, 226.7, 204.0 and 173.9 mAh g^{-1}. Maximum specific capacity electrode is obtained using the 3S-V_2O_5 HoMSs/ Ni-Cotton. This is attributed to the fact that a larger surface area can be provided by 3S-V_2O_5 HoMSs and more active sites for lithium-ion storage, so specific capacity can be improved. Also, when compared with V_2O_5 nanosheets, HoMSs materials shown better cyclic stability and capacity, that is mainly due to some of the factors. Firstly, because of the pore structure, electrolyte permeates the inner shell better. Secondly, the thin shell reduces the stress caused by volume expansion and reduction, while also shortens the time needed for transportation Thirdly, multi-shell structures may provide more places to store lithium.

2.3. Orthorhombic phase V_2O_5 with O vacancies (denoted as V- V_2O_5)

V-V_2O_5 is also an appealing material available for use in lithium battery cathode. **Figure 4.** are SEM, TEM images showing pure V_2O_5 and V- V_2O_5. From the graph provided, it is clear that both V-V_2O_5 and V_2O_5 have two-dimensional lamellar morphology. Using higher magnification SEM and TEM images, V-V_2O_5 has many deeper troughs on the surface and large surface fluctuations (**Figure 4. c, g**, **h**), whereas V_2O_5 is a slab fracture attributable to mechanical forces during sample preparation (**Figure 4. f, j**, **k**), the rough surface of V- V_2O_5 more effectively inhibits the accumulation of flakes, stores more electrolytes, provides more material-electrolyte contact area, and loosens mechanical strain resulting from insertion/disinsertion cycle of Li^+ compared with pure V_2O_5 [9].

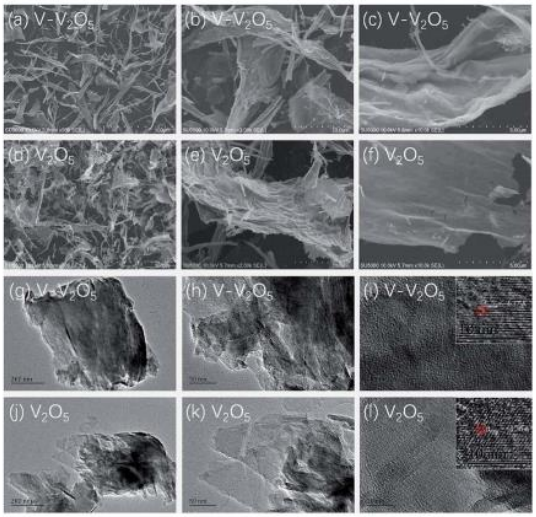

Figure 4. SEM, TEM samples of V_2O_5 and V-V_2O_5[9]

According to Sun et al., at the current density of 200 mA g^{-1}, **Figure 5.** a shows the cyclic ability for both the V-V_2O_5 and the pure V_2O_5 electrode. Compared with pure V_2O_5, it is clear that V-V_2O_5 shows better discharge capacity. Given current density of 1A g^{-1} (**Figure 5.** c), maximum specific discharge capacity of V-V_2O_5 and V_2O_5 is respectively 230.2 and 256.6 mAh g^{-1}. The discharge capacity after 50 cycles are respectively 213.1 and 237.9 mAh g^{-1}, and the discharge capacity after 100 cycles are respectively 199.2 and 224.7 mAh g^{-1}.0Insertion/ removal capacity of Lithium ions in V- V_2O_5 are always better compared with traditional V_2O_5. The capacity retention rate of V-V_2O_5 still remains at 87.6% at the 100th cycle. Even at higher current density of 3A g^{-1}, as shown in **Figure 5.** d, excellent discharge capacity stability is still shown on the graph, always higher than that of V_2O_5, and remain at the value for approximately 150 mAh g^{-1} for all the cycle number smaller than 200.

Cyclic stability of V_2O_5 and V-V_2O_5 samples is compared for 1 and 3 g^{-1} current density (**Figure 5.** c, d). At 1A g^{-1}, there is first increased and then decreased discharge capacity of V-V_2O_5 and V_2O_5, the maximum capacity are found to be 218.4 and 200.6 mAh g^{-1}. During cycle measurement, the significant increase in capacity during the first few cycles can be attributed to electrode activation (electrolyte penetration and/or active surface increase). After 200 cycles, discharge capacities of V- V_2O_5 and V_2O_5 are respectively to be 189.3 and 172.4 mA h^{-1}. When 3A g^{-1} is adopted, the capacity first increased slowly and remained stable for both two electrodes. Maximum discharge capacities of V_2O_5 and V-V_2O_5 are respectively 141.7 and 150 mAh g^{-1}. In the condition of hypoxia, V_2O_5 is easy to lose the O atom in crystal structure and form Oxygen vacancy. O vacancies acts as important role to help to reduce V^{5+} to V^{4+}, improve electron and ionic conductivity, also providing additional sites for lithium ions to embed in [10-11].

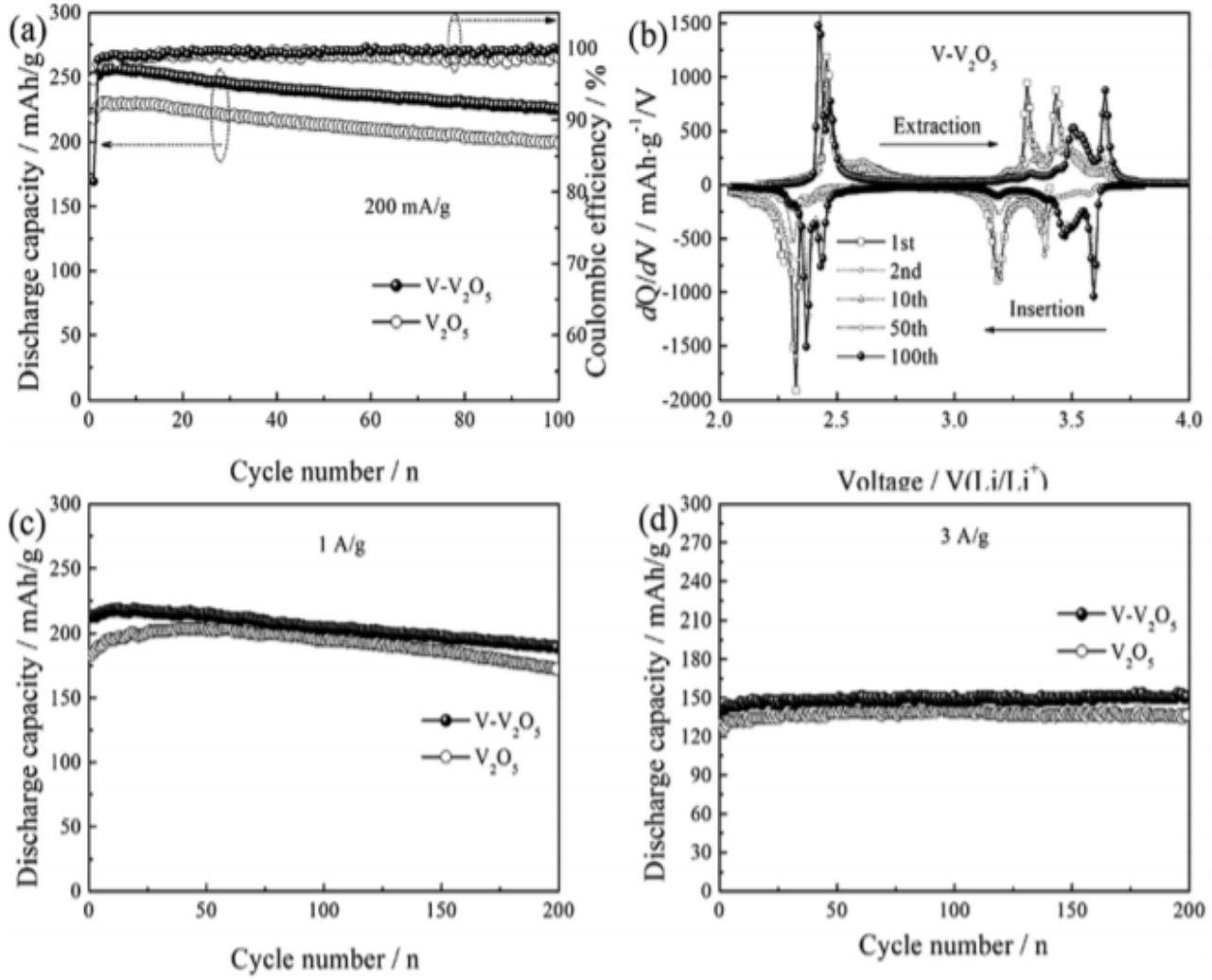

Figure 5. (a) V- V_2O_5 and V_2O_5 electrodes at a current density of 200 mA g^{-1}, measured for the cyclic performance; (b) At a current density of 200 mA g^{-1}, differential specific capacity plots of the V- V_2O_5 drawn with different cycle numbers, cyclic performance of V-V_2O_5 and V_2O_5, respectively, are drawn at a current density of (c) 1 A g^{-1} and (d) 3 A g^{-1} [9].

2.4. Li_2O-V_2O_5-SiO_2-B_2O_3 glass

Suitable cathode materials also include glass materials because of their controllable capacity by controlling the composition of the glass. In addition, glass materials ordered with short-range structure can have much improved dynamics, and facilitate electrochemical cycling.

SiO_2 has a very high melting point (1650±50°C), so for the Li_2O-V_2O_5-SiO_2 glass system, there is also a higher melting point. Therefore, a low melting point (450°C) B_2O_3 glass molding agent was used to reduce the melting point. In addition, because of phase separation, borosilicate glass has high ionic conductivity, and B_2O_3 can also reduce the tendency of crystallization in terms of the glass material.

In **Figure 6.**, $20Li_2O$-$30V_2O_5$-(50-x)SiO_2-xB_2O_3 (x=10, 20, 30, 40) are named as LVSB10, LVSB20, LVSB30 and LVSB40 sample, respectively. The two graphs provide evidence for the cyclic stability for these cathode materials. **Figure 6.** a and b shows the relationship between voltage and discharge capacity. Under both circumstances, 50 mAh g^{-1} density is adopted. It is find that under the 1.5V to 4.2V voltage range, four samples display poor capacity of charging. The discharge capacities of LVSB10, LVSB20, LVSB30 and LVSB40 were 123.7 mAh g^{-1}, 51.5 mAh g^{-1}, 37.9 mAh g^{-1} and 19.5 mAh g^{-1}, respectively.

With high V^{4+} ratio, in the LVSB10 sample, it has higher initial discharge capacity compared with that in other samples. Plus, the more number of V^{4+}, the smaller polaron jump can be generally shown, thus achieving higher conductivity [12].

However, the capacity of the glass cathode material decreases rapidly. The capacities of all four LVSB materials undergoes rapid decrease after 50 cycles. The capacity retention rates were hardly above 50%, showing not stable cyclability when more charge and recharge cycles are being repeated. In **Figure 6.** b, the results shows that LVSB glass has electrochemical activity, but poor cycling performance for glass cathode material, mainly caused by the low electron conductivity due to the large particle size and its volume may also have changed during the ion and electron extraction or insertion.

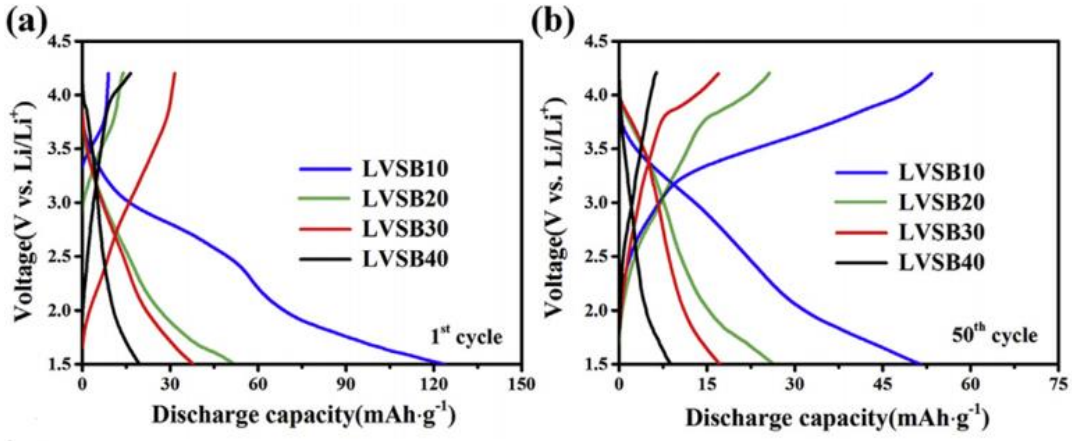

Figure 6. Charge and discharge curves for (a) 1st cycle, (b) 50th cycle using LVSB10, LVSB20, LVSB30 and LVSB40 as glass samples [12].

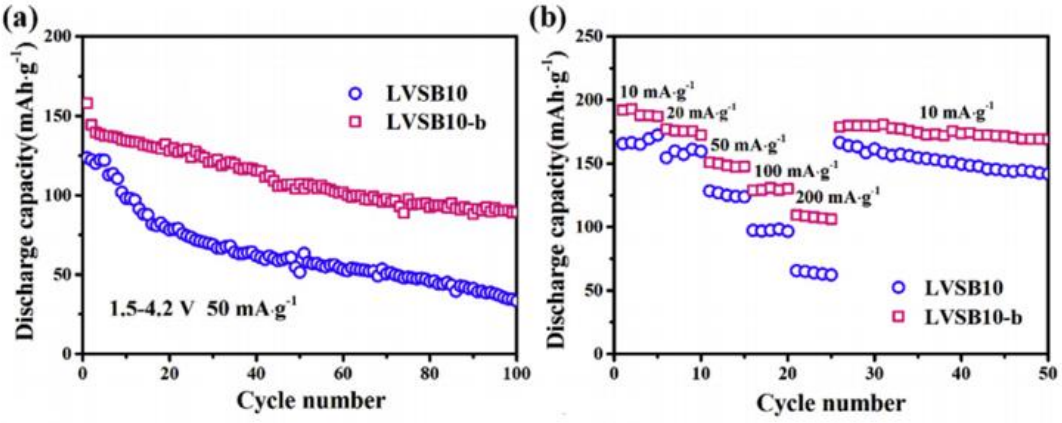

Figure 7. Cycle number versus discharge capacity of LVSB and LVSB-b for both fixed current density(a) and changing ones (b)

LVSB10-b can be made by milling the LVSB 10 sample, which this process can make LVSB 10 particle smaller, creating LVSB10-b with smaller particle. Cyclability ability of both LVSB and LVSB 10-b are first going to pass through a stable voltage, which ranges from 1.5V to 4.2V to give stable current density of 50 mA g^{-1}. In this case, it can be shown from **Figure 7.** a that LVSB 10-b obviously win in every cycle number under 100 in terms of discharge capacity. For the 100^{th} cycle, LVSB 10-b still reaches discharge capacity of approximately 100 mAh g^{-1}, still maintain the capacity retention of nearly 70%, while the value for LVSB of discharge capacity at 100^{th} cycle is only approximately 30 mAh g^{-1}. In **Figure 7.** b, providing the changing current density, LVSB 10-b still shows better performance under the condition of different current density. The main increase in cyclability is mainly due to the impedance of charge transfer

is largely decreased, and lithium ion diffusion is rather easier. It is conjectured that due to the decrease in particle size for LVSB 10-b, both electron and lithium ion transporting pathways can be shortened, so the conductivity of the cathode can be effectively improved.

2.5. V_2O_5 xerogel

V_2O_5 xerogel can be directly made from traditional V_2O_5 crystals. The xerogel is obtained by adding molten vanadium oxide that is heated to 800°C into water. According to Huguenin et al., [13] the electrochemical performance analysis showed that V_2O_5 xerogel was a suited lithium battery cathode material choice, with a reduction potential 3 higher than that of lithium, an energy density of about 600 Wh kg^{-1}, and a specific capacity of about 250 Ah kg^{-1}. However, the poor cyclability that decreases obviously with the increase of the number of cycles for vanadium oxide xerogel still exists.

film	annealing gas	interlayer spacing (Å)	grain size (nm)
1	3 h air	11.0	14.3
2	0.5 h air +2.5 h N_2	11.1	11.6
3	2.5 h N_2 + 0.5 h air	11.2	6.4
4	3 h N_2	11.5	5.1

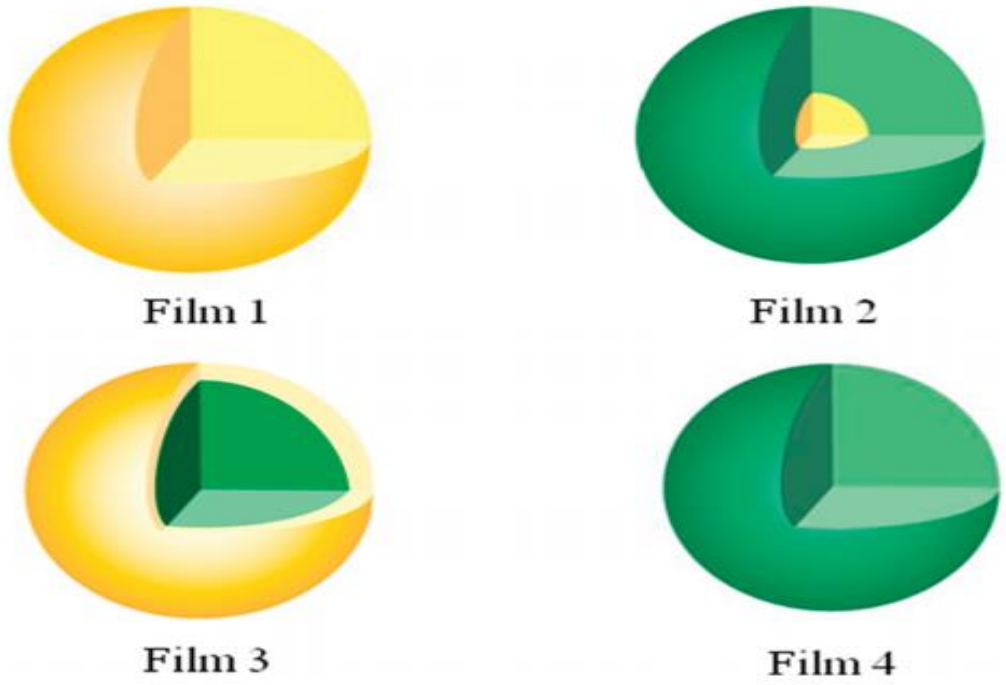

Figure 8. Different composition of V_2O_5 films, which are annealed with varying N_2 and air composition. Presence of V^{5+}(yellow) and V^{4+}(green) can also be known from the graph [13]

Four films can be derived from the vanadium oxide xerogel in terms of different composition, as shown in **Figure 8.** on the left. These four films have different grain sizes and also have different chemical properties. Reduction is induced by N annealing, causing yellow V^{5+} ions to green V^{4+} ion. As shown in the graph, in film 1, there is no or very little V^{4+}; in film 2, V^{4+} ions (green exterior) covers the surface of the film. There is many V^{4+} ions inside the film 3 (green), but due to re-exposure to air, V^{4+} on the surface of the film is oxidized to V^{5+}; There are V^{4+} ions in film 4 as in film 3, but because only N_2 annealing is

applied, there is no V^{4+} reoxidation on the surface [13].

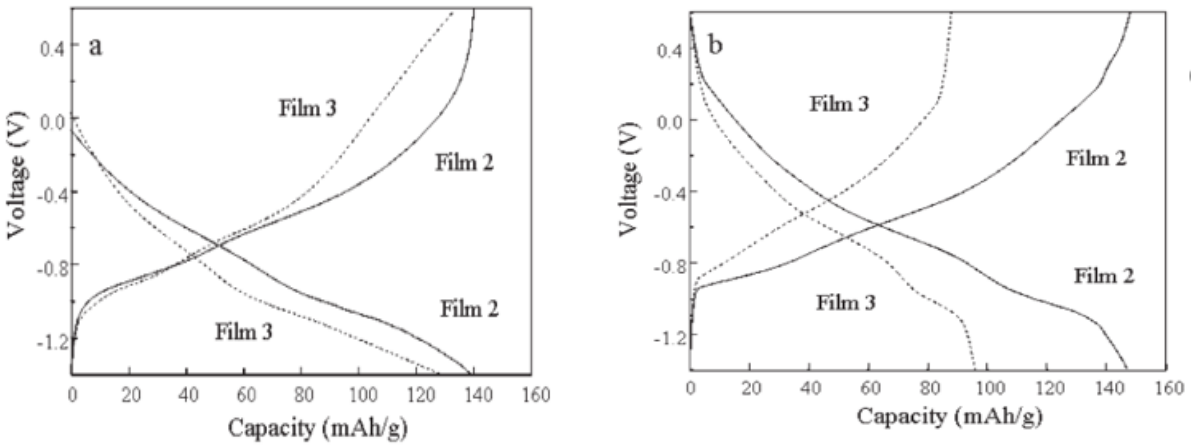

Figure 9. Films 2 and film 3 under 600 mA g^{-1} current density of V_2O_5 at (a) 1st (b) 30th cycles for air and N_2 condition at 300 degrees Celsius for 3 hours (0.6V to 1.4V) [13]

Figure 9. is the graph that shows at the constant current density for 600mA g^{-1}, the voltage-capacity relationship for the first and 30th CP curves. In Figure 9a, the initial CP curves of film 2 and film 3 start at ~ -0.07 V and ~ 0.03 V, respectively. Compared with air-annealed films, the charge-discharge curves of both films are inclined and have clearer platform. Because of the intercalation mechanism of the solution, film 2 with low crystallinity has the discharge capacity of 139 and 137 mAh g^{-1}, and that of film 3 is respectively 129 and 133 mAh g^{-1}. However, what is appealing is that film 2 actually shows very small irreversible capacity for only 2mAh g^{-1}. This proved film 2 to have very good reversibility. In **Figure 9.** b, for the 30th cycle, film 2 also displays very small irreversibility for only 1mAh g^{-1}, while that of film 3 reaches 8mAh g^{-1}. Using these data, we can conclude that in contrast with film 3, which degrades its capacity seriously within 30 cycles, film 2 shows very good coulomb efficiency with little irreversible capacity, and also better discharge capacity.

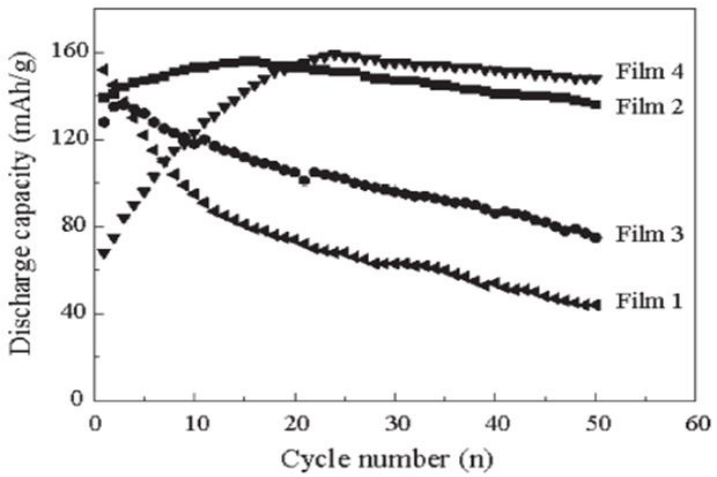

Figure 10. Discharge capacity versus cycle number for all the 4 films, with same condition applied in **Figure 9.** [13]

In **Figure 10.**, the discharge capacity versus cycle number graph is drawn in order to show the four film's stability in discharge capacity maintenance. Under the condition of 600mA g^{-1} current density condition for 50 cycle numbers, film 2 in the four lithium ion intercalated films displays best cyclic stability.

With an initial around 140mAh g^{-1}, capacity, its capacity slightly improved in the following several cycles, and reach a maximum discharge capacity for cycle number 15, and then followed by a mild decline after 15 cycles. At cycle number 15, the capacity still remains high at 136 mAh g^{-1}, which shows very high coulomb efficiency for approximately 98 percent. Film 4 also display similar cyclability properties. Discharge capacity rise relatively fast with cycle number at first, with initial value about 68 mAh g^{-1}. Although a sightly decline follows after around 24 cycles, final discharge capacity after 50 cycles still reaches 148 mAh g^{-1}. Film 3 shows good initial discharge capacity, but it decreases fast and after 50 cycles it only reaches 75 mAh g^{-1}, which is quite low with maintenance of about 60% of initial value. Capacity degradation of film 1 is more severe. According to Liu, et al, the advantage in film 2 is found attributed to both more surface defects as well as larger size of grains. In contrast, for film 3, it is opposite with film 2 with less surface defects, but smaller size of grain. Both film 2 and film 4 have surface defects, their good performance shows the existence of surface defect is very essential for a good cyclic stability.

2.6. Aniline polymer (PANI)

The combination with aniline polymer creates new path that are parallel to vanadium oxide chain, and largely adds convenience for the transport of electrons. There exists space charge effect between PANI chain, which serves as conductive phase, and vanadium oxide itself. The chains are held together by the increased interface area created by hydrogen bonding (NH—OV) between vanadium oxide and PANI, resulting in a greater effect on the electron conductivity [13].

$$x(C_6H_5NH_2) + V_2O_5 + (y/2)O_2 \rightarrow (C_6H_4NH)_xV_2O_5^{(2x-2y)-} + yH_2O + (2x-2y)H^+$$

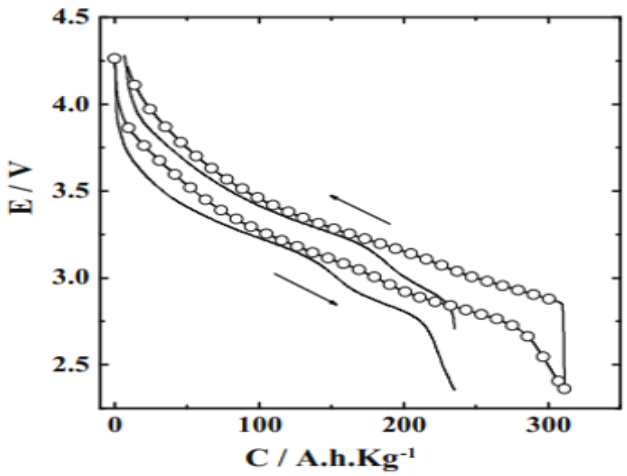

Figure 11. In condition of 0.5M $LiClO_4$, the Chronopotentiometric curves for $[PANI]_{0.3}V_2O_5$ (line with circle) and V_2O_5 (solid line) [14]

As shown in **Figure 11.**, V_2O_5/PANI shows better ability of lithium ion diffusion, and compared to the normal V_2O_5 xerogel, it also has better conductivity of electrons. That is caused by the better charge capacity (313 Ah kg^{-1} for $[PANI]_{0.3}V_2O_5$ and 234 Ah kg^{-1} for V_2O_5) [14]. Huguenin et al. also find that in the condition of $[PANI]0.3V_2O_5$, Lithium ions are the easiest to diffuse in the battery. More results show that when the molar ratio of PANI is 30%, the capacity ratio of V2O5/PANI nanofibers is stable at about 300 mAh g^{-1}. The morphology of V_2O_5/PANI did not change significantly after 10 charges and discharges, but structural defects were found when only nanostructures were used.

3. Conclusion

In conclusion, it is found that the various derivatives for the original V_2O_5 compound are found to have promising implication possibilities. Most of the improvement focus on how to increase the diffusion of ions and electron in those cathode materials and the surface defects vacancies in order to increase the diffusion rate and to increase its capacity, while improvements are also made in order for increasing cyclability performance over charges and discharges. Samples such as V_2O_5 xerogel are easier to made while also have a better performance in terms of cyclability and discharge capacity. LVSB-10b combines vanadium oxide into glass compound and also shows promising future developments. Best ratio of these derived vanadium oxide compounds has also been discovered in terms of composition in cathode to maximize their performance. It is believed that V_2O_5 will achieve more developments in the near future and be able to play an important role in lithium battery cathode.

Disclosure statement

The author declares no conflict of interest.

References

[1] Hatchard TD, Dahn JR, 2004, J. Electrochem. Soc, 151(6): A838.

[2] Marom R, Amalraj SF, Leifer N, et al., 2011, A Review of Advanced and Practical Lithium Battery Materials. Journal of Materials Chemistry, 21(27): 9938-9954.

[3] Karapidakis E, Vernardou D. n.d., Topic review Vanadium Oxides Subjects, Chemistry, Applied View times: 18.

[4] Tomaszewska A, Chu Z, Feng X, et al., 2019, Lithium-ion Battery Fast Charging: A Review. E Transportation, 1: 100011.

[5] Gu, Gang, et al., 2003, "V_2O_5 Nanofibre Sheet Actuators." Nature Materials, 2(5): 316-319.

[6] Gamze Y, Chun X, Lu, 2016, "High-Performance Solid-State Supercapacitors Based on V_2O_5/Carbon Nanotube Composites." Chem Electro Chem, 3(1): 158-164.

[7] Zhu Y, et al., 2020, "V_2O_5 Textile Cathodes with High Capacity and Stability for Flexible Lithium-Ion Batteries." Advanced Materials, 32(7): 1906205.

[8] Sun Y, Xie Z, Li Y, 2018, "Enhanced Lithium Storage Performance of V_2O_5 with Oxygen Vacancy." RSC Advances, 8(69): 39371-39376.

[9] Khemchand D, et al., 2012, "Synthesis and Characterization of Self-Assembled Nanofiber-Bundles of V_2O_5: Their Electrochemical and Field Emission Properties." Nanoscale, 4(2): 645-651.

[10] Roberta V, et al., 2018, "On the Strange Case of Divalent Ions Intercalation in V_2O_5." Journal of Power Sources, 407: 162-172.

[11] Zhao EL, et al. 2019, "Electrochemical Performance of Li_2O-V_2O_5-SiO_2-B_2O_3 Glass as Cathode Material for Lithium Ion Batteries." Journal of Materiomics, 5(4): 663-669.

[12] Liu D, et al., 2011, "Enhanced Lithium-Ion Intercalation Properties of V_2O_5 Xerogel Electrodes with Surface Defects." The Journal of Physical Chemistry C, 115(11): 4959-4965.

[13] Huguenin F, Martins AR, Torresi RM, 2018, Nanocomposites from V_2O_5 and Lithium-Ion Batteries. In Nanoenergy, Springer, Cham, 223-249.

[14] Huguenin F, Torresi RM, Buttry DA, 2002, Lithium Electro-Insertion into an Inorganic-Organic Hybrid Material Composed from V_2O_5 and Polyaniline, J Electrochem Soc, 149: A546.